Nanoscale

RSC Publishing

PAPER

View Article Online
View Journal | View Issue

Mechanics of rolling of nanoribbon on tube and sphere†

Cite this: *Nanoscale*, 2013, **5**, 5450

Qifang Yin and Xinghua Shi*

The configuration of graphene nano-ribbon (GNR) assembly on carbon nanotube (CNT) and sphere is studied through theoretical modeling and molecular simulation. The GNR can spontaneously wind onto the CNT due to van der Waals (vdW) interaction and form two basic configurations: helix and scroll. The final configuration arises from the competition among three energy terms: the bending energy of the GNR, the vdW interaction between GNR and CNT, the vdW between the GNR itself. We derive analytical solutions by accounting for the three energy parts, with which we draw phase diagrams and predict the final configuration (helix or scroll) based on the selected parameters. The molecular simulations are conducted to verify the model with the results agree well with the model predicted. Our work can be used to actively control and transfer the tube-like nanoparticles and viruses as well as to assemble ribbon-like nanomaterials.

Received 28th January 2013
Accepted 5th April 2013

DOI: 10.1039/c3nr00489a

www.rsc.org/nanoscale

1 Introduction

Graphene nanoribbons (GNRs), with outstanding properties inherited from graphene,[1,2] have promising potential applications in innovative electronics.[3–5] The fabrication of high quality GNR thus becomes the key for its industrial application. Several methods have been developed to fabricate GNRs with desired edges, including the self-assembly of fullerenes within a single-walled carbon nanotube (CNT)[6] and unzipping of multi-walled CNTs.[7] Enthusiasm for the fabrication aside, one crucial problem worth being studied is the assembly of GNRs. It has been found the aspect ratio of GNR directly influences its configuration[8–11] which may have negative effect on the applications. It is thus desirable to explore an effective method to control the assembly of GNR. Through molecular dynamics (MD) simulations a few approaches have been proposed.[10–14] For instance, some works obtain repetitively folded and knots-grouped GNRs in which the GNRs are transformed from simple ribbons into complicated structures.[10,11] Some utilize CNTs to initiate the assembly of GNRs,[12–14] and find that GNRs interact with the CNT in various ways, such as encapsulation inside the CNTs helically[13,14] and formation of a carbon nanoscroll (CNS) outside the CNT.[12] These works have paid much attention on the assembly process of GNRs, while the mechanism determining the final configurations remains largely unexplored. For example, it remains elusive under which situation the GNR would form scroll around the CNT. It is desirable to explore a theoretical model to predict the final configuration of GNRs. In this letter we focus on the interaction of a GNR on both single-walled and multi-walled CNTs and a sphere. We derive an analytical solution to predict the final configuration (helix or scroll) of GNR around the CNT/sphere based on the selected parameters. We also conduct MD simulations to verify the predictions. We note that our work can also be extended to actively control or transfer the tube-like nanoparticles and viruses *via* nanoribbon as well as to assemble ribbon-like nanomaterials.

LNM, Institute of Mechanics, Chinese Academy of Sciences, Beijing, 100190, P. R. China. E-mail: shixh@imech.ac.cn

† Electronic supplementary information (ESI) available. See DOI: 10.1039/c3nr00489a

2 Interaction between a GNR and a tube

2.1 Theoretical model

When a GNR with length L and width b winding on the surface of CNT with radius r_0, the total potential energy of the system can be expressed as

$$E = W + \Gamma \tag{1}$$

where W and Γ are the elastic bending energy and the total interfacial energy between GNR–CNT and GNR–GNR. They can be expressed as

$$\Gamma = \gamma A \tag{2}$$

$$W = \frac{D}{2r_0^2} A \tag{3}$$

where γ is the interfacial energy per unit area, A is the area of interface and D the bending rigidity of GNR. The interfacial energy is integrated from 6–12 Lennard–Jones potential $E_0 = 4\varepsilon\left[\left(\frac{\sigma}{t}\right)^{12} - \left(\frac{\sigma}{t}\right)^{6}\right]$ in the condition of continuity assumption, where ε and σ are Lennard–Jones parameters and t the distance between two atoms. To simplify the mathematical manipulation, the scroll is assumed to be formed by concentric

circles with radii r_i (i = 1, 2,…N).[15] Therefore the interfacial energy per unit area can be expressed as

$$\gamma(r_i, r_j, \varepsilon) = \gamma_{i,j} = \lambda(r_i, r_j)\varepsilon = \lambda_{i,j}\varepsilon \quad (4)$$

where

$$\lambda_{i,j} = \frac{3}{2}\pi\rho_1\rho_2 r_i r_j \left[\frac{21}{32}\left(\frac{\sigma}{r_j}\right)^{12} I\left(\frac{r_i}{r_j}, \frac{11}{2}\right) - \left(\frac{\sigma}{r_j}\right)^{6} I\left(\frac{r_i}{r_j}, \frac{5}{2}\right)\right], (r_j > r_i), \quad (5)$$

$$I(p,q) = \int_0^{2\pi} \left(1 + p^2 - 2p\cos\phi\right)^{-q} \mathrm{d}\phi, \quad (6)$$

ρ_1 and ρ_2 are the density of carbon atoms of the two interfacial surfaces, and r_i and r_j are the radii of the selected two concentric circles, respectively. As shown in Fig. 1, we mark r_0 as the radius of the CNT. For multi-walled CNT, we mark r_0 as the radius of outermost wall, r_{-1} as the radius of second outermost wall, and so on. The interlayer space $d = r_i - r_{i-1}$, (i = 1, 2, 3,…N), is considered to be a constant d = 3.4 Å.

We note that the interfacial energy decays quickly with the increase of layer interval. To see how fast the decaying is, we numerically calculated the parameter $\lambda_{i,j}$ ($i,j = -1, 0, 1, 2, 3,\ldots$) with eqn (5), where $j - i = 1$ for the interaction between two adjacent layers, $j - i = 2$ for the interaction between one layer and its second nearest layer, $j - i = 3$ for the interaction between one layer and its third nearest layer, and so on. With r_i = 5 nm, we find $\lambda_{i,i+2} = 0.1004\lambda_{i,i+1}$ and $\lambda_{i,i+3} = 0.0194\lambda_{i,i+1}$. So as $j - i = 2$, the interaction between one layer and its second nearest layer is about 10% of that for two adjacent layers, while as $j - i = 3$, the interaction between one layer and its third nearest layer is only about 2% of that for adjacent layers. To simplify our model we ignore the contribution from $\lambda_{i,i+3}$ and thereafter.

In the scroll configuration, the interfacial energy exists not only between the CNT and GNR, but also between GNR itself as well. As a scroll is treated as concentric circles, the calculation of energies of a scroll is thus simplified. The total potential energy (interfacial and bending) of the i-th ring could be expressed as

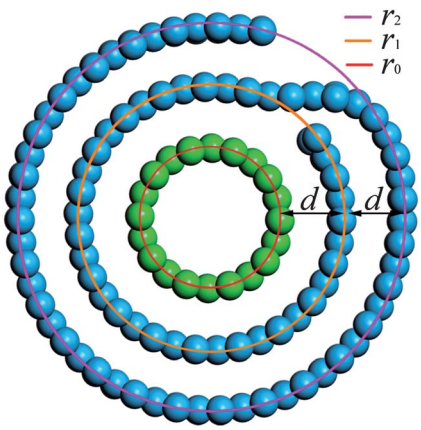

Fig. 1 The schematic display of a CNS (cyan) winding around a CNT (green).

$$E_{Si} = 2\pi r_i b\left(\gamma_{i-2,i} + \gamma_{i-1,i}\right) + \frac{\pi bD}{r_i} \quad \text{for } i > 1, \quad (7)$$

and

$$E_{S1} = 2\pi r_1 b\left(\gamma_{0,1} + \gamma_{-1,1}\right) + \frac{\pi bD}{r_1} \quad \text{for } i = 1, \quad (8)$$

where $\gamma_{0,1} = \lambda_{0,1}\varepsilon_{t\text{–}g}$, $\gamma_{-1,1} = \lambda_{-1,1}\varepsilon_{t\text{–}g}$ and $\gamma_{0,2} = \lambda_{0,2}\varepsilon_{t\text{–}g}$ are the interfacial energies per unit area between the GNR and CNT's walls. $\varepsilon_{t\text{–}g}$ is the LJ parameter for the interaction between tube and graphene. As i >1, $\gamma_{i-1,i} = \lambda_{i-1,i}\varepsilon_{g\text{–}g}$ and $\gamma_{i-2,i} = \lambda_{i-2,i}\varepsilon_{g\text{–}g}$, where $\varepsilon_{g\text{–}g}$ is the LJ parameter for the interaction between graphenes. Here the interfacial energy between i-th ring and (i + 1)-th ring (and thereafter) is not accounted in to avoid repetitive counting.

If the i-th ring is transformed into helix on the same CNT, the potential energy of this ring is

$$E_{Hi} = 2\pi r_i b\left(\gamma_{0,1} + \gamma_{-1,1}\right) + \frac{\pi bDr_i}{{r_1}^2} \quad \text{for } i > 1, \quad (9)$$

and

$$E_{H1} = 2\pi r_1 b\left(\gamma_{0,1} + \gamma_{-1,1}\right) + \frac{\pi bD}{r_1} \quad \text{for } i = 1. \quad (10)$$

Note that $E_{S1} = E_{H1}$.

The total potential energy of the entire scroll and helix could be described by

$$E_S = n_1E_{S1} + n_2E_{S2} + n_3E_{S3} + \ldots = n_1E_{S1} + \sum_{i>1} n_iE_{Si}, \quad (11)$$

and

$$E_H = n_1E_{H1} + n_2E_{H2} + n_3E_{H3} + \ldots = n_1E_{H1} + \sum_{i>1} n_iE_{Hi}, \quad (12)$$

where $n_i = 1$ for a complete ring and $0 < n_i < 1$ for an incomplete one. If $0 < n_i < 1$ then $n_{i+1} = n_{i+2} = \ldots = 0$. The length of the GNR could be written in a form as

$$L = 2\pi r_1 n_1 + 2\pi r_2 n_2 + 2\pi r_3 n_3 + \ldots = \sum_{i=1} 2\pi r_i n_i. \quad (13)$$

Eqn (12) then can be recast into

$$E_H = \left(\gamma_{0,1} + \gamma_{-1,1} + \frac{D}{2{r_1}^2}\right) bL. \quad (14)$$

Note that E_H has linear relationship with the length L.

Let $E_S = E_H$, the solution of the equation would be the sets of parameters which determine the final configuration of GNR on CNT: helix or scroll. This equation leads to

$$\sum_{i=2}^{N} n_i \left[2r_i\left(\gamma_{i-2,i} + \gamma_{i-1,i} - \gamma_{0,1} - \gamma_{-1,1}\right) + \frac{D}{r_i} - \frac{Dr_i}{{r_1}^2}\right] = 0, \quad (15)$$

or

$$\sum_{i=1}^{N} n_i \left[2\pi r_i\left(\gamma_{i-2,i} + \gamma_{i-1,i}\right) + \frac{\pi D}{r_i}\right] - \left(\gamma_{0,1} + \gamma_{-1,1} + \frac{D}{2{r_1}^2}\right) L = 0. \quad (16)$$

Eqn (16) relates the tube radius with the length of GNR. It sets the marginal situation of the final configuration of GNR.

For a simplified case where $N = 2$ and $L = 2\pi(r_1 + r_2)$. Then eqn (15) leads to

$$\gamma_{0,1} + \gamma_{-1,1} + \frac{D}{2}\frac{1}{{r_1}^2} = \gamma_{0,2} + \gamma_{1,2} + \frac{D}{2}\frac{1}{{r_2}^2}. \quad (17)$$

For the case of GNR rolling onto a single-walled CNT, eqn (17) leads to

$$\gamma_{0,1} + \frac{D}{2}\frac{1}{{r_1}^2} = \gamma_{0,2} + \gamma_{1,2} + \frac{D}{2}\frac{1}{{r_2}^2}. \quad (18)$$

Eqn (17) and (18) show that, if parameters (r_0, ε_{t-g}, ε_{g-g}) are solutions of the equation, both helix and scroll configurations have the same energy state. For those parameters which do not satisfy the eqn (17) and (18), the configuration would tend to be scroll if $E_S < E_H$ and helix if $E_S > E_H$.

Normalize eqn (17) and (18) we obtain eqn (19)

$$\frac{\varepsilon_{t-g}}{\varepsilon_{g-g}} = \frac{1}{\lambda_{0,2} - \lambda_{0,1} - \lambda_{-1,1}}\left[\frac{D}{2\varepsilon_{g-g}d^2}\left(\frac{1}{(x+1)^2} - \frac{1}{(x+2)^2}\right) - \lambda_{1,2}\right] \quad (19)$$

for GNR rolling on multi-walled CNT and

$$\frac{\varepsilon_{t-g}}{\varepsilon_{g-g}} = \frac{1}{\lambda_{0,2} - \lambda_{0,1}}\left[\frac{D}{2\varepsilon_{g-g}d^2}\left(\frac{1}{(x+1)^2} - \frac{1}{(x+2)^2}\right) - \lambda_{1,2}\right] \quad (20)$$

for GNR rolling on single-walled CNT, where $x = \frac{r_0}{d}$. Eqn (19) and (20) relates the ratio between the interaction of tube–graphene and graphene–graphene with the geometric parameter of CNT. It sets the marginal situation of the final configuration of GNR.

2.2 Molecular dynamics (MD) simulation

To verify the theoretical model we conduct MD simulations using package LAMMPS.[16] A GNR is selected with width (along armchair direction) of 12.564 Å and length (along zigzag direction) of about $L = 2\pi(r_0 + d) + 2\pi(r_0 + 2d)$. The C–C bonds in the GNR are described by the Adaptive Intermolecular Reactive Empirical Bond Order (AIREBO) Potential,[17] and the LJ parameters between GNR itself are fixed as $\varepsilon_{g-g} = 0.00284$ eV and $\sigma_{g-g} = 3.4$ Å. A series of zigzag CNTs (m,0) with different radius ($m = 10, 12, 14, 16, 18, 20, 25, 35, 45, 130$) are constructed. The parameter of σ_{t-g} for LJ potential between CNT and GNR is equal to σ_{g-g} and ε_{t-g} is varied. The density of carbon atoms ρ_t and ρ_g are both 0.3950 Å^{-2}. In MD simulations, we first generated helix and scroll structures (Fig. 2) with specific LJ parameters in which NVT ensemble was used and temperature was controlled at 10 K. The boundary condition was non-periodic. For helix configuration the interval between edges of GNR are set farther than the cutoff of LJ potential so that there are no interactions among them (Fig. 2a). Based on the obtained structures, we changed the LJ parameter ε and minimize the system energy by conjugate gradient algorithm. When the minimized energy for helix structure is equal to that of scroll structure at specific ε, then this ε is what we needed to separate the two regions of helix and scroll. In MD simulation the edges of GNR have unignorable contribution to the system energy,[13,18] which is not taken into account in the theoretical model. To eliminate the edge effect in MD simulation to accord with the theoretical model, we construct two GNRs with widths $2b$ and b to form helixes. The energy difference between the potential energy of the two helixes is then chosen as the final potential energy of the system in which the edge effect is eliminated during the subtraction. The same methodology is also used in the case of scroll.

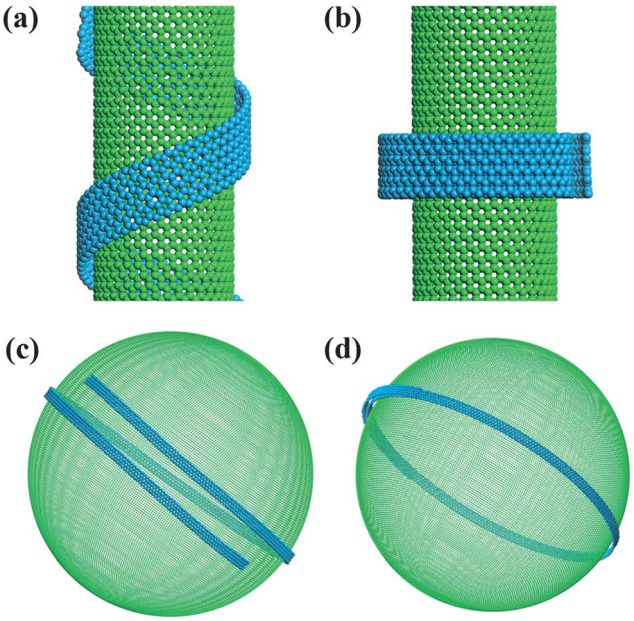

Fig. 2 The helix and scroll configurations of GNR on CNT and sphere. (a) Helix on CNT with chirality (45,0). (b) Scroll on CNT with chirality (45,0). (c) Helix on sphere. (d) Scroll on sphere.

We note that the torsional energy in the helix form is not taken into account in the theoretical model. According to our MD simulation (see ESI†) we find this term has ignorable contribution to the total strain energy, and omit it in the model for simplification.

2.3 Results and discussions

Fig. 3a shows the normalized potential energies for scroll and helix configurations around CNT as a function of length of GNR (normalized by tube radius) which are described by eqn (11) and (12), respectively. It is seen that if the LJ parameter $\varepsilon_{t-g} = 0.004$ eV, the potential energy for scroll would become lower than that of

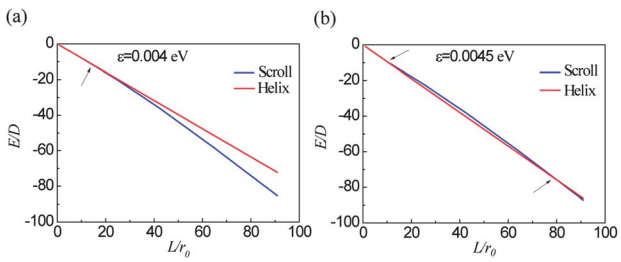

Fig. 3 The potential energy of scroll/helix as a function of length of GNR. The radius of CNT r_0 is fixed to 5.388 Angstrom and the LJ parameter ε_{t-g} is (a) 0.004 eV and (b) 0.0045 eV. The bending stiffness of the GNR $D = 1.2$ eV.[19]

helix after the first layer rolling; for a larger LJ parameter ε_{t-g} = 0.0045 eV (Fig. 3b), the potential energy for scroll would be first higher after first layer rolling, then lower than that of helix. It indicates that as a ribbon is long enough, the potential energy of scroll would be always lower than that of helix. And the final configuration of GNR should be scroll.

With eqn (16), the phase diagram is drawn in Fig. 4 indicating how the radius of tube and length of GNR influence the final configuration of GNR. The red line sets the margin at which the potential energy forming the scroll and helix is the same. The region above the red line means the energy state of scroll configuration is lower than the helix so the scroll formation is preferred. And it is opposite beneath the red line.

For a short GNR, the final configuration is dependent on the interfacial LJ parameter ε_{t-g}. To see how the ε_{t-g} influences the final configuration of short GNR, we select the special case described in eqn (19) and (20). Fig. 5a indicates how the interfacial energy and the radius of the tube influence the final configuration of GNR into scroll or helix. The red and magenta lines set the margin at which the potential energy forming the scroll and helix is the same. The region above the line means the energy state of helix configuration is lower than that of scroll so the helix formation is preferred. And it is opposite beneath the line. It means the formation of helix always needs more tube–graphene interfacial energy than that of scroll. It could be understood that during the winding of GNR, the elastic bending energy density in scroll decreases because of the increase of radius, while for helix it keeps constant. We note that the line descends with the increase of tube radius, which means given fixed interfacial energy of tube–graphene, the formation of GNR can be a scroll with a small tube while a helix with a large one. For instance, with $\varepsilon_{t-g}/\varepsilon_{g-g} = 1.4$, the GNR would form scroll with $r_0/d = 1$ while it would form a helix with $r_0/d = 4$. Also if the tube is multi-walled, the marginal line falls down due to the additional CNT–GNR interaction.

The circles and triangles in Fig. 5a are the MD results separating the two regions. It is seen that for GNR winding on large tube, the MD results agree with the theoretical prediction well. For small tube, MD results have ~10% deviation from the theoretical one. We attribute this inconsistency to the concentric circles assumption for the scroll in our theoretical modeling, which inevitably underestimates the length of scroll

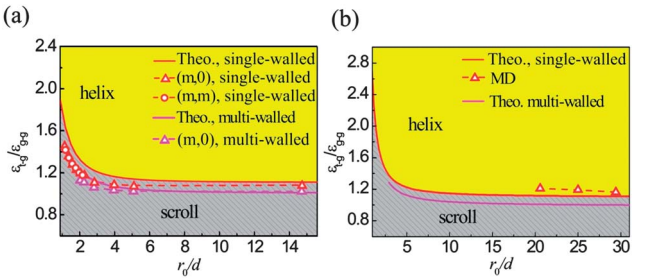

Fig. 5 Phase diagram of the configuration of GNR in the space of tube–graphene interaction and size of (a) CNT, (b) sphere. The red (for single-walled) and magenta (for multi-walled) lines are the marginal ones on which the energy states of both helix and scroll are equal. The circles in (a) are results from MD simulations with chirality of CNT (*m*,*m*) and the triangles with chirality (*m*,0). The triangles in (b) are the MD results.

as the tube is small. The variation of bending rigidity of graphene at large curvature,[20] the continuity assumption in theoretical model may also have contributions here.

To investigate the influence of chirality, simulations with CNT of (*m*,*m*) (*m* = 6, 7, 8, 9, 10, 11) are performed and the results are plotted in Fig. 5a. It is shown that chirality has ignorable effects.

To further investigate how the number of rolling layers, *N*, or the length of GNR, *L*, influences the phase diagram as shown in Fig. 5a, we change the parameter of *N* in the theoretical model and draw additional phase diagram. From Fig. 6 it is seen that as *N* increases, the level curves lift up, indicating the initially formed helix configuration would transform into scroll as more GNR winding onto the CNT. However such transformation may not occur spontaneously due to the energy barrier. Such a kinetics related problem is out of current scope and we will leave it for further study elsewhere.

3 Interaction between a GNR and a sphere

3.1 Theoretical model

Besides the interaction of GNR on CNT, we also studied the interaction of GNR on a sphere. Following the procedure as the theoretical calculation of GNR on CNT, we deduce an equation influencing the final configuration of GNR on sphere

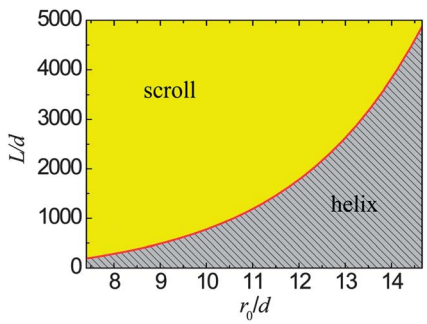

Fig. 4 The relation between the length of GNR and the radius of CNT. The points on red line are geometrical parameters with which the potential energies of helix and scroll are equal. The LJ parameter ε_{t-g} = 0.0032 eV.

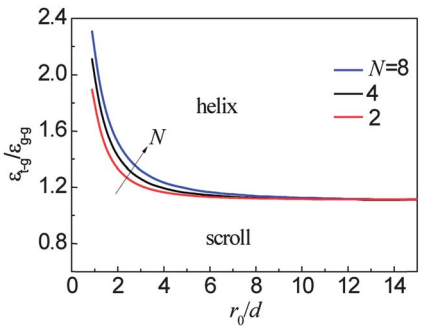

Fig. 6 Variation of the level curves in the phase diagram as the number of concentric circles, *N*, increases.

$$\sum_{i=2}^{N} n_i \left[2r_i\left(\gamma_{i-2,i} + \gamma_{i-1,i} - \gamma_{0,1} - \gamma_{-1,1}\right) + \frac{D}{r_i} - \frac{Dr_i}{r_1^2} \right] = 0, \quad (21)$$

which has the same form as eqn (15). Eqn (21) has presumed that the GNR sticks onto the sphere surface tightly without wrinkles, which needs $r_0 \gg b$. At the same time, we ignore the energy induced by the compressing and/or twisting of the GNR when it is interacting with the sphere. Here:

$$\lambda_{i,j} = 16\rho_1\rho_2 r_i^2 \left[\left(\frac{\sigma}{r_j}\right)^{12} I\left(\frac{r_i}{r_j}, 6\right) - \left(\frac{\sigma}{r_j}\right)^{6} I\left(\frac{r_i}{r_j}, 3\right) \right], (r_j > r_i), \quad (22)$$

$$I(p,q) = \int_0^{\frac{\pi}{2}} \cos\theta \mathrm{d}\theta \int_0^{\pi} \left(1 + p^2 - 2p\cos\theta\cos\phi\right)^{-q} \mathrm{d}\phi. \quad (23)$$

Let $N = 2$, we have the same equations as eqn (19) and (20), which can be used to describe the interactions between a GNR and a sphere.

3.2 MD simulation

MD simulations are conducted to verify the theoretical model for sphere. A GNR with width (along armchair direction) of 8.376 Å and length (along zigzag direction) of 651.651 Å is selected to interact respectively with spheres with radii of 70, 85, 100 Å. The atoms are distributed on the surface of the sphere as evenly as possible. The LJ parameters between GNR itself are the same as those in the previous simulations while the parameter of σ_{s-g} for LJ potential between the sphere and GNR is equal to σ_{g-g} and ε_{s-g} is varied. The density of atoms ρ_g is 0.3950 $Å^{-2}$ and ρ_s is 0.4032 $Å^{-2}$.

Fig. 5b shows how the interfacial energy and the radius of sphere influence the configuration of GNR when $N = 2$. Note that under the condition $r_0 \gg b$ the region where x is small is of less significance. The MD result can agree with the theoretical prediction as the radius of sphere is large. It deviates from theoretical prediction as the radius decreases, which is attributed to the breakdown of the assumption of $r_0 \gg b$.

4 Conclusion

In summary, to study two basic configurations of the GNR on tube/sphere, helix and scroll, we developed a theoretical model to describe the interactions between GNR and tube/sphere, in which elastic energy of the GNR, interfacial energy among the GNR itself, and interfacial energy between GNR and tube/sphere are considered. Phase diagrams are presented to determine the parameters influencing the formation of scroll/helix which include the length of GNR, the geometry of the tube/sphere as well as the interfacial energy among the GNR and the tube/sphere. The theoretical model indicates that given fixed interfacial energy of tube–graphene or sphere–graphene, the GNR can wind into scroll with small tube/sphere or a helix with large tube/sphere. We then performed MD simulations to verify the theoretical model with results agreeing well with the theoretical prediction. Our work can be used to actively and precisely control the assembling or transferring of nanoribbons.

Acknowledgements

The work is supported by the National Natural Science Foundation of China (NSFC) (Grant no. 11023001 and 11272327) and computation is mainly supported by the Supercomputing Center of Chinese Academy of Sciences (SCCAS).

References

1 K. S. Novoselov, A. K. Geim, S. V. Morozov, D. Jiang, Y. Zhang, S. V. Dubonos, I. V. Grigorieva and A. A. Firsov, Electric field effect in atomically thin carbon films, *Science*, 2004, **306**, 666.
2 C. Lee, X. Wei, J. W. Kysar and J. Hone, Measurement of the elastic properties and intrinsic strength of monolayer graphene, *Science*, 2008, **321**, 385.
3 L. Yang, C. H. Park, Y. W. Son, M. L. Cohen and S. G. Louie, Quasiparticle energies and band gaps in graphene nanoribbons, *Phys. Rev. Lett.*, 2007, **99**, 186801.
4 V. Barone, O. Hod and G. E. Scuseria, Electronic structure and stability of semiconducting graphene nanoribbons, *Nano Lett.*, 2006, **6**, 2748.
5 H. Zhao, K. Min and N. R. Aluru, Size and chirality dependent elastic properties of graphene nanoribbons under uniaxial tension, *Nano Lett.*, 2009, **9**, 3012.
6 A. Chuvilin, E. Bichoutskaia, M. C. Gimenez-Lopez, T. W. Chamberlain, G. A. Rance, N. Kuganathan, J. Biskupek, U. Kaiser and A. N. Khlobystov, Self-assembly of a sulfur-terminated graphene nanoribbon within a single-walled carbon nanotube, *Nat. Mater.*, 2011, **10**, 687.
7 L. Jiao, L. Zhang, X. Wang, G. Diankov and H. Dai, Narrow graphene nanoribbons from carbon nanotubes, *Nature*, 2009, **458**, 877.
8 K. V. Bets and B. I. Yakobson, Spontaneous twist and intrinsic instabilities of pristine graphene nanoribbons, *Nano Res.*, 2009, **2**, 161.
9 Z. Xu and M. J. Buehler, Geometry controls conformation of graphene sheets: membranes, ribbons, and scrolls, *ACS Nano*, 2010, **4**, 3869.
10 B. V. C. Martins and D. S. Galvão, Curved graphene nanoribbons: structure and dynamics of carbon nanobelts, *Nanotechnology*, 2010, **21**, 075710.
11 A. L. J. Pang, V. Sorkin, Y. W. Zhang and D. J. Srolovitz, Self-assembly of free-standing graphene nano-ribbons, *Phys. Rev. A: At., Mol., Opt. Phys.*, 2012, **376**, 973.
12 Z. Zhang and T. Li, Carbon nanotube initiated formation of carbon nanoscrolls, *Appl. Phys. Lett.*, 2010, **97**, 081909.
13 N. Patra, Y. Song and P. Kral, Self-assembly of graphene nanostructures on nanotubes, *ACS Nano*, 2011, **5**, 1798.
14 Y. Jiang, H. Li, Y. Li, H. Yu, K. M. Liew, Y. He and X. Liu, Helical encapsulation of graphene nanoribbon into carbon nanotube, *ACS Nano*, 2011, **5**, 2126.
15 T. Wang, C. Zhang and S. Chen, Mechanical behaviors of carbon nanoscrolls, *J. Nanosci. Nanotechnol.*, 2012, **12**, 1.

16 S. Plimpton, Fast parallel algorithms for short-range molecular dynamics, *J. Comput. Phys.*, 1995, **117**, 1.
17 S. J. Stuart, A. B. Tutein and J. A. Harrison, A reactive potential for hydrocarbons with intermolecular interactions, *J. Chem. Phys.*, 2000, **112**, 6472.
18 Z. Guo, T. Chang, X. Guo and H. Gao, Thermal-induced edge barriers and forces in interlayer interaction of concentric carbon nanotubes, *Phys. Rev. Lett.*, 2011, **107**, 105502.
19 Q. Lu, M. Arroyo and R. Huang, Elastic bending modulus of monolayer graphene, *J. Phys. D: Appl. Phys.*, 2009, **42**, 102002.
20 T. Ma, B. Li and T. Chang, Chirality- and curvature-dependent bending stiffness of single layer graphene, *Appl. Phys. Lett.*, 2011, **99**, 201901.